Efficient Invariant-Manifold, Low-Thrust Planar Trajectories to the Moon ⋆

Giorgio Mingotti * **Francesco Topputo** **
Franco Bernelli-Zazzera **

* *Institut für Industriemathematik, Universität Paderborn, Warburger Str. 100, 33098 Paderborn, Germany (e-mail: mingotti@math.upb.de).*
** *Dipartimento di Ingegneria Aerospaziale, Politecnico di Milano, Via La Masa 34, 20156 Milano, Italy ({topputo,bernelli}@aero.polimi.it)*

Abstract: Two-impulse trajectories as well as mixed invariant-manifold and low-thrust efficient transfers to the Moon are discussed. Exterior trajectories executing ballistic lunar capture are formalized through the definition of special attainable sets. The coupled restricted three-body problems approximation is used to design appropriate first guesses for the subsequent optimization. The introduction of the Moon-perturbed Sun-Earth restricted three-body problem allows to formalize the idea of ballistic escape from the Earth and to take explicitly advantage of lunar fly-by. Then, accurate first guess solutions are optimized, through a direct method approach and multiple shooting technique.

Keywords: Nonlinear astrodynamics; N-body problems; Low-energy trajectories; Dynamical system theory; Low-thrust propulsion; Optimal control theory.

1. INTRODUCTION

Low energy transfers to the Moon are being studied since the rescue of the Japanese spacecraft Hiten in 1991 Belbruno and Miller (1993). In essence, a low energy lunar transfer reduces the hyperbolic excess velocity upon Moon arrival, typical of a patched-conics approach. This process is called ballistic capture, and relies on a better exploitation of the gravitational nature ruling the transfer problem instead of the classic Keplerian decomposition of the solar system. The reduced speed relative to the Moon sets the trajectory to low energy levels, which in turn imply a reduced propellant mass needed to stabilize the spacecraft around the Moon.

In this paper, both efficient two-impulse transfers and the low-thrust version of the transfers described in Koon et al. (2001) are presented, all of them starting from the same LEO with an impulsive maneuver given by the launcher. It is in fact possible to further reduce the propellant necessary to send a spacecraft to the Moon by exploiting both the simultaneous gravitational attractions of the Sun, the Earth, and the Moon, and the high specific impulse provided by the low-thrust engines (above 1000 seconds). Nevertheless, including the low-thrust is not trivial, and asks for a number of issues to face. It is of great importance, for instance, overcoming the loss of Jacobi integral, finding subsets of the phase space that lead to low-thrust ballistic capture (playing the separatrix-like role of the stable manifold associated with $L2$ Lyapunov orbit of the Earth–Moon system), and summarizing, using as few parameters as possible, all the reachable orbits that it is possible to target with the finite thrust magnitude available, like low lunar orbits LLOs.

The purpose of this work is therefore to formulate a systematic approach for the design of efficient pure low-energy as well as mixed invariant-manifold low-thrust transfers to low orbits around the Moon. Then, a comparison between the trajectories computed and some solutions found in literature is presented.

2. DESIGN STRATEGY

With the *coupled restricted three-body problems approximation*, the four-body dynamics, characterizing the low energy lunar transfers, is decomposed into two RTBPs, and the invariant manifolds of the Lyapunov orbits are computed. It is possible to show that, with a suitably chosen Poincaré section, the trajectory design is restricted to the selection of a single point on this section Koon et al. (2001).

The transfers studied in this work are defined as follows. The spacecraft is assumed to be initially on a circular parking orbit around the Earth at a height $h_E = 167\,\mathrm{km}$; then an impulsive maneuver, Δv_E, carried out by the launch vehicle, places the spacecraft on a translunar trajectory, performing a translunar insertion TLI. Two different typologies of mission are investigated, with respect to the propulsion adopted: (i) low-energy two-impulse transfers to LLOs: after the insertion, the spacecraft flies ballistically under the dynamics of the problem until the Moon neighborhood, where a second impulsive maneuver inserts it on a stable low altitude orbit; (ii) low-energy low-thrust transfers to LLOs: after the launch, the spacecraft can only rely on its low-thrust propulsion to reach a stable low-altitude orbit around the Moon.

⋆ AstroNet - Marie Curie Research Training Network. European Community's Sixth Framework Programme.

2.1 The Planar Circular Restricted Three-Body Problem

The motion of the spacecraft, m_3, is studied in the gravitational field generated by the mutual circular motion of two primaries of masses m_1, m_2, respectively, about their common center of mass. It is assumed that m_3 moves in the same plane of m_1, m_2 under the following equations Szebehely (1967):

$$\ddot{x} - 2\dot{y} = \frac{\partial \Omega}{\partial x}, \qquad \ddot{y} + 2\dot{x} = \frac{\partial \Omega}{\partial y}, \tag{1}$$

where the auxiliary function is

$$\Omega(x, y, \mu) = \frac{1}{2}(x^2 + y^2) + \frac{1-\mu}{r_1} + \frac{\mu}{r_2} + \frac{1}{2}\mu(1-\mu), \tag{2}$$

and $\mu = m_2/(m_1+m_2)$ is the mass parameter of the three-body problem. (1) are written in a barycentric rotating frame with nondimensional units: the angular velocity of m_1, m_2, their distance, and the sum of their masses are all set to the unit value. It is easy to verify that the primary of mass $1-\mu$, is located at $(-\mu, 0)$, whereas the smaller primary μ, is located at $(1-\mu, 0)$; thus, the distances between m_3 and the primaries are:

$$r_1^2 = (x+\mu)^2 + y^2, \qquad r_2^2 = (x+\mu-1)^2 + y^2. \tag{3}$$

For fixed μ, the Jacobi integral reads

$$J(x, y, \dot{x}, \dot{y}) = 2\Omega(x, y, \mu) - (\dot{x}^2 + \dot{y}^2), \tag{4}$$

and, for a given energy C, it defines a three-dimensional manifold

$$F(C) = \{(x, y, \dot{x}, \dot{y}) \in \mathcal{R}^4 | J(x, y, \dot{x}, \dot{y}) - C = 0\}, \tag{5}$$

foliating the four-dimensional phase space.

3. EARTH ESCAPE STAGE

If a value of Jacobi constant in the SE model, C_{SE}, is suitably chosen, there exists a unique Lyapunov orbit about both $L1$ and $L2$, labeled γ_1 and γ_2, respectively. Assuming the energy values $C_{SE} \ll C_2$ such that both γ_1 and γ_2 exist, the Hill's regions are opened at both $L1$ and $L2$. Without any loss of generality, the Earth escape stage is constructed considering the dynamics around $L2$; using $L1$ instead of $L2$ is straightforward. The stable and unstable manifolds associated with γ_2, $W^s(\gamma_2)$ and $W^u(\gamma_2)$, are computed starting from the Lyapunov orbit until a certain surface of section is reached.

Aiming at exploiting the structure of both $W^s(\gamma_2)$ and $W^u(\gamma_2)$, two surfaces of section are introduced to study their cuts at different stages. Section S_A, making an angle φ_A (clockwise) with the x-axis and passing through the Earth, is considered to cut $W^s(\gamma_2)$, whereas section S_B, inclined by φ_B (counterclockwise) on the x-axis and passing through the Earth, is assumed for $W^u(\gamma_2)$.

Candidate trajectories for Earth–Moon transfers are non-transit orbits close to both $W^s(\gamma_2)$ and $W^u(\gamma_2)$. This property is wanted since the existence of $W^s(\gamma_2)$ and $W^u(\gamma_2)$ has to be exploited, although the transfer orbit does not exactly lie on any invariant subset. Let $\dot{\Gamma}_2^s$ be the set of points in the $(r_2, \dot{r}_2)$-plane that are enclosed by $\partial\Gamma_2^s$, and $\bar{\Gamma}_2^s$ the closed set made up of $\partial\Gamma_2^s \cup \dot{\Gamma}_2^s$. Points on $\bar{\Gamma}_2^s$ have to be avoided as they lead to either transit or asymptotic orbits. On the contrary, all the points that lie on

$$l = \{(r_2, \dot{r}_2) \in S_A,\ (r_2, \dot{r}_2) \notin \bar{\Gamma}_2^s | r_2 = R_E + h_E\} \tag{6}$$

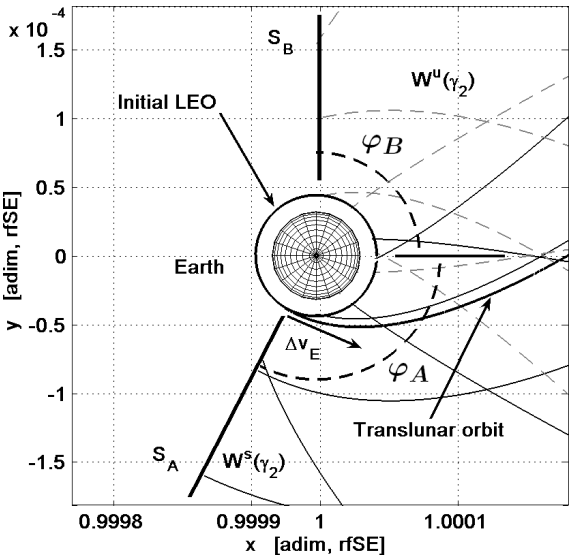

(a) Initial transfer condition.

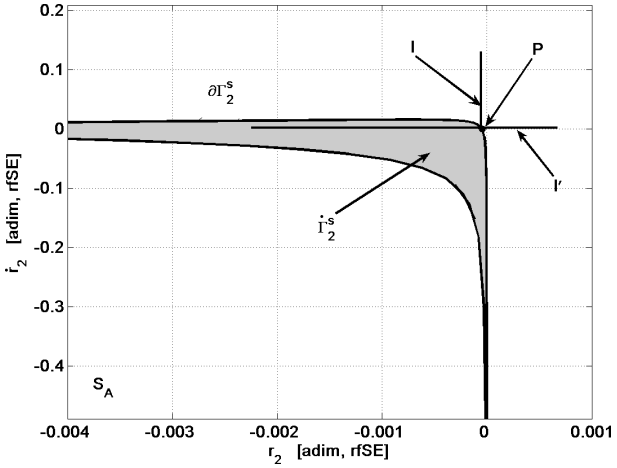

(b) $\partial\Gamma_2^s$, $\dot{\Gamma}_2^s$, l, l' sets, and point $P = l \cap l'$.

Fig. 1. Earth escape trajectory performed with a tangential Δv_E maneuver and its associated section point P.

are translunar candidate orbits as they intersect the initial parking orbit (R_E is the radius of the Earth). This intersection occurs in the configuration space only, as the initial parking orbit and the translunar trajectory have two different energy levels.

The pair $\{C_{SE}, \varphi_A\}$ uniquely defines the curve $\partial\Gamma_2^s$ on S_A: C_{SE} stands for the orbit γ_2, whereas φ_A defines the surface of section S_A to cut the first intersection of $W^s(\gamma_2)$. Thus, $\{C_{SE}, \varphi_A\}$ are used to define the first guess Earth escape stage. In order to obtain efficient transfer trajectories, the lowest possible initial instantaneous maneuver, Δv_E, is searched. It is necessary to define its components: a first contribution to the Δv_E amount is related to the radial term Δv_r, while the second tangential contribution Δv_t is needed to fill the gap ΔC between the energy of the initial parking orbit, C_E, and C_{SE} (i.e. $\Delta C = C_E - C_{SE}$). It is possible to show that $\Delta v(\Delta C, \varphi_A) = \Delta v_t(\Delta C) + \Delta v_r(\varphi_A)$, and it is even possible to lower Δv_r to zero by properly tuning φ_A. This approach leads to initial tangential maneuvers, i.e. the initial Δv_E is aligned with the velocity of the circular parking orbit around the Earth. The search is therefore restricted to the point $P \in S_A$

defined by $P = l \cap l'$, where l' is the set of points having zero radial velocity with respect to the Earth

$$l' = \{(r_2, \dot{r}_2) \in S_A,\, (r_2, \dot{r_2}) \notin \bar{\Gamma}_2^s | \dot{r}_2 = 0\}. \quad (7)$$

Point P does not exactly lie on the stable manifold (but outside), and can be found sufficiently close to $W^s(\gamma_2)$ by suitably tuning φ_A (see Fig. 1(b)). In particular, points $P' \in S_A$ such that $\|P' - P\| \leq \varepsilon$ are also taken into account, where ε is a certain prescribed distance.

The set labeled $\mathcal{E}_{SE}$, $\mathcal{E}_{SE} \in S_B$, stands for the set of orbits close to $W^u(\gamma_2)$ whose pre-image $\mathcal{E}_{SE}^{-1}$, $\mathcal{E}_{SE}^{-1} \in S_A$, is made up by P' points.

3.1 The Moon-Perturbed Sun-Earth Restricted Three-Body Problem

When the gravitational attraction of the Moon is taken into account, (1) are augmented aiming at introducing the dynamics of the Moon in an autonomous fashion, leading to the formulation of the bicircular restricted four-body problem, BRFBP (see Fig. 2(a)). The dynamical system moves from the fourth order to the fifth one. Some assumptions are taken into account, recalling that the orbits of the primaries show low eccentricity values (≈ 0.01, ≈ 0.04), and the Moon inclination with respect to the ecliptic plane is little ($\approx 5\,\text{deg}$).

Assuming all the hypothesis written above, the planar equations of motion are:

$$\ddot{x} - 2\dot{y} = \frac{\partial \Omega_M}{\partial x}, \qquad \ddot{y} + 2\dot{x} = \frac{\partial \Omega_M}{\partial y}, \qquad \dot{\theta} = \omega_M \quad (8)$$

where the subscripts denote the partial derivative of the auxiliary function

$$\Omega_M(x, y, \theta) = \Omega(x, y, \mu_{SE}) + \frac{m_M}{r_M} - \frac{m_M}{\rho_M^2}\,(x\cos\theta + y\sin\theta). \quad (9)$$

The quantity $\Omega(x, y, \mu_{SE})$ stands for the classic CRTBP potential expressed by (2), while the remaining part represents the gravitational perturbation of the Moon.

The dimensionless physical constants introduced to describe the Moon influence are in agreement with those of the SE model. Thus, the distance between the Moon and the Earth is $\rho_M = 2.5721 \cdot 10^{-3}$, the mass of the Moon is $m_M = 3.6942 \cdot 10^{-8}$, and its angular velocity with respect to the SE rotating frame is $\omega_M = 1.2367 \cdot 10^{1}$. The location of the Moon is therefore at $(1 - \mu_{SE} + \rho_M \cos\theta, \rho_M \sin\theta)$, such that:

$$r_M^2 = (x - 1 + \mu_{SE} - \rho_M \cos\theta)^2 + (y - \rho_M \sin\theta)^2. \quad (10)$$

According to the differential (8), the system does not admit the existence of any libration point or integral of motion. Anyway, as the Moon can be considered as a small perturbation of the Sun–Earth model, a qualitative global analysis about the motion of the spacecraft is proposed, assuming the restricted four-body model as a perturbation of the invariant objects of the classic RTBP. If the points belonging to the escape set $\mathcal{E}_{SE}$ are backwards integrated under the dynamics associated with (8), the topology of their trajectories in the configuration space is only slightly and negligible different. The main variations appear associated with the pre-image set $\mathcal{E}_{SE}^{-1}$. If the trajectories pass nearby the Moon, the points $P' \in S_A$ show almost the same phase-space coordinates $(r_2, \dot{r}_2)$ as before, while the tangential velocity decreases significantly, with respect to the classic Sun–Earth PCRTBP computation. This means that a reduced instantaneous velocity change Δv_E is now required to place the translunar trajectory on $F(C_{SE}) \cap \mathcal{E}_{SE}^{-1}$.

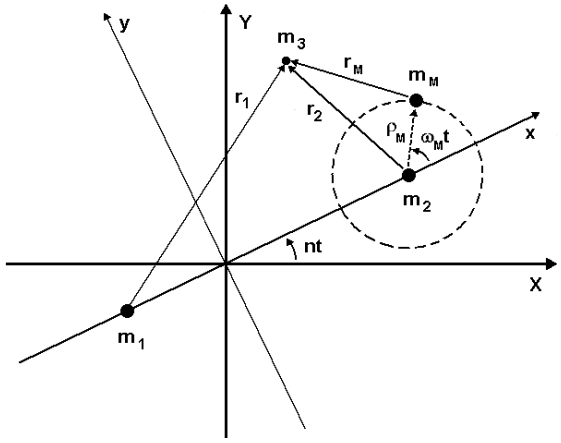

(a) Moon-perturbed Sun–Earth RTBP.

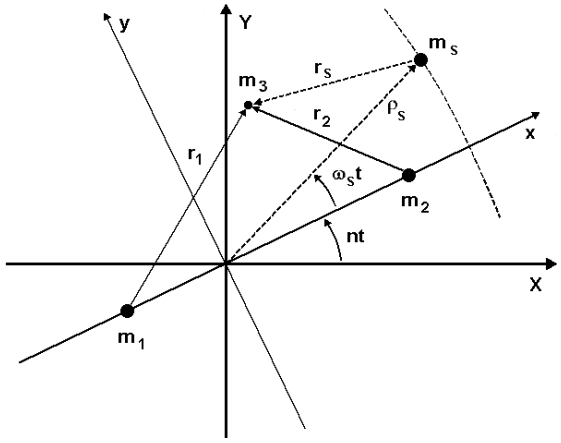

(b) Sun-perturbed Earth–Moon RTBP.

Fig. 2. Mathematical models to described the physics of the problem.

4. LOW-THRUST AND ATTAINABLE SETS

To model the *controlled* motion of m_3 under both the gravitational attractions of m_1, m_2, and the low-thrust propulsion, the following differential equations are considered:

$$\ddot{x} - 2\dot{y} = \frac{\partial \Omega}{\partial x} + \frac{T_x}{m}, \quad \ddot{y} + 2\dot{x} = \frac{\partial \Omega}{\partial y} + \frac{T_y}{m}, \quad \dot{m} = -\frac{T}{I_{sp}\, g_0}, \quad (11)$$

where $T = \sqrt{T_x^2 + T_y^2}$ is the thrust magnitude, I_{sp} the specific impulse of the engine and g_0 the gravitational acceleration at sea level. The ballistic motion (1) is represented by a fourth-order system, while the controlled motion (11) is described by a fifth-order system of differential equations. Continuous variations of the spacecraft mass, m, are taken into account when low-thrust propulsion is considered.

The thrust law $\mathbf{T}(t) = \{T_x(t), T_y(t)\}^\top$, $t \in [t_i, t_f]$, in (11) is not given, but rather in this approach it represents an unknown that is found when the optimal control

problem is solved (t_i and t_f are the initial and final times, respectively). Let $\mathbf{y}_i$ be a vector representing a generic initial state, i.e. $\mathbf{y}_i = \{x_i, y_i, \dot{x}_i, \dot{y}_i, m_i\}^\top$, and let $\phi_{\mathbf{T}(\tau)}(\mathbf{y}_i, t_i; t)$ be the flow of system of (11) at time t, starting from $(\mathbf{y}_i, t_i)$ and considering the thrust profile $\mathbf{T}(\tau)$, $\tau \in [t_i, t]$. The latter has to be taken within proper bounds that are typically given by technological constraints. This condition usually reads $T(t) \leq T_{max}$, where T_{max} is the maximum available thrust magnitude. With this notation, it is possible to define the generic point of a tangential low-thrust trajectory through

$$\mathbf{y}(t) = \phi_{\overline{\mathbf{T}}}(\mathbf{y}_i, t_i; t), \tag{12}$$

where $\overline{\mathbf{T}} = \overline{T}(\mathbf{v}/v)$, $v = \sqrt{\dot{x}^2 + \dot{y}^2}$, $\mathbf{v} = \{\dot{x}, \dot{y}\}^\top$. (12) represents the flow of the differential system governed by (11), when constant tangential thrust of magnitude $\overline{T}$ is considered. With given $\overline{T}$, tangential thrust maximizes the variation of Jacobi energy, which is the only property that has to be dealt with when designing trajectories in the RTBP. The low-thrust orbit, at time t, can be expressed as

$$\gamma_{\overline{\mathbf{T}}}(\mathbf{y}_i, t) = \{\phi_{\overline{\mathbf{T}}}(\mathbf{y}_i, t_i; \tau) | \tau < t\}, \tag{13}$$

where the dependence on the initial state $\mathbf{y}_i$ is kept. The attainable set, at time t, can be defined as

$$\mathcal{A}_{\overline{\mathbf{T}}}(t) = \bigcup_{\mathbf{y}_i \in \mathcal{Y}} \gamma_{\overline{\mathbf{T}}}(\mathbf{y}_i, t), \tag{14}$$

where $\mathcal{Y}$ is a domain of admissible initial conditions.

4.1 Moon Ballistic Capture Stage

Two-impulse transfers to the Moon are defined as follows. The spacecraft is assumed to be initially on a parking orbit about the Earth with given eccentricity and perigee altitude. The transfer begins when the spacecraft is at the perigee of this orbit by means of an impulsive maneuver (provided by the launcher). Then the spacecraft flies ballistically under the RTBP dynamics until it reaches the Moon neighborhood, where a second impulsive maneuver is required to insert the spacecraft into a stable prescribed orbit around the Moon. The transfer terminates when the spacecraft is at the periapsis of this orbit.

The initial orbit is a trajectory belonging to the set $\mathcal{E}_{SE}$, whereas the second part is defined using a suitable attainable set in the EM model. This set is made up by ballistic orbits that are integrated backward, i.e. considering the thrust magnitude $T = 0$. More specifically, the final state of the transfers (i.e., the periapsis point of the orbit about the Moon) is function of the argument of periapsis and of the final tangential Δv_M impulsive maneuver required to place the spacecraft into a stable lunar orbit, i.e. $\mathbf{y}_f = \mathbf{y}_f(\omega_M, \Delta v_M)$, see Fig. 3(a).

According to this approach, the domain of admissible final states becomes

$$\mathcal{Y}^M = \{\mathbf{y}_f(\omega^M, \Delta v_M) | \omega_M \in [0, 2\pi], \Delta v_M \in [0, +\infty]\}, \tag{15}$$

and the attainable set, for some $t \geq 0$ (i.e. $-t$ is a backward integration), containing ballistic capture trajectories with impulsive stabilization is

$$\mathcal{A}^M_{\mathbf{B}}(-t) = \bigcup_{\mathbf{y}_f \in \mathcal{Y}^M} \gamma_{\mathbf{B}}(\mathbf{y}_f(\omega_M, \Delta v_M), -t). \tag{16}$$

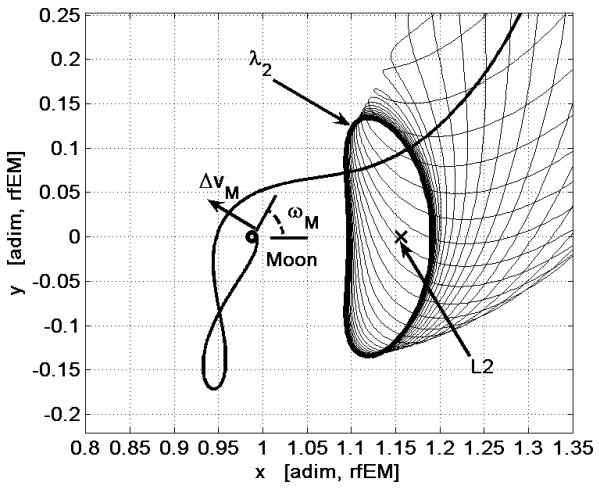

(a) Sample impulsive capture trajectory.

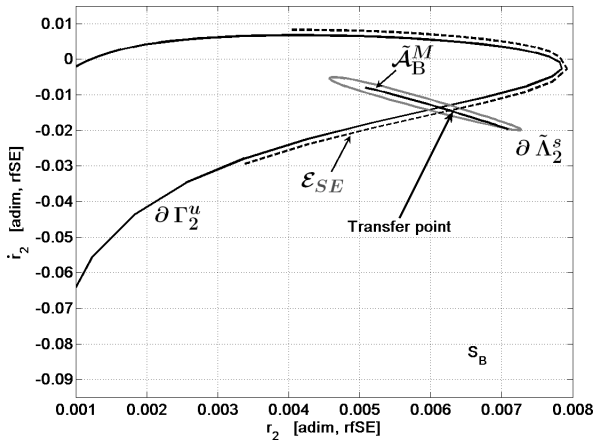

(b) $\mathcal{E}_{SE}$ and $\tilde{\mathcal{A}}^M_{\mathbf{B}}(-t)$ sets.

Fig. 3. The first guess impulsive capture solution as the transfer point $\mathcal{B}^M_{-t} = \mathcal{E}_{SE} \cap \tilde{\mathcal{A}}^M_{\mathbf{B}}(-t)$, the latter reported on section S_B in Fig. 3(b).

Each generic Moon capture orbit written in (16), at time $-t$, can be expressed as

$$\gamma_{\mathbf{B}}(\mathbf{y}_i, -t) = \{\phi_{\mathbf{B}}(\mathbf{y}_i, t_i; -\tau) | -\tau > -t\}, \tag{17}$$

where $\mathbf{B} = T(\mathbf{v}/v)$, $v = \sqrt{\dot{x}^2 + \dot{y}^2}$, $\mathbf{v} = \{\dot{x}, \dot{y}\}^\top$, and assuming $T = 0$. Since the first part of the transfer is defined on $\mathcal{E}_{SE}$, the transfer points, if any, that generate two-impulse transfers are contained in the set

$$\mathcal{B}^M_{-t} = \mathcal{E}_{SE} \cap \tilde{\mathcal{A}}^M_{\mathbf{B}}(-t). \tag{18}$$

Once again, the transformation $\mathcal{M}$ is required to map $\mathcal{A}^M_{\mathbf{B}}(-t)$, computed in the EM model, into $\tilde{\mathcal{A}}^M_{\mathbf{B}}(-t)$, defined in the SE model, see Fig. 3(b). At this stage just first guesses are defined, states with small, tolerable mismatches can be admitted in $\mathcal{B}^M_{-t}$ as the discontinuities are spread in the subsequent optimization step.

4.2 Moon Low-Thrust Capture Stage

Low-energy, low-thrust transfers to the Moon, have the same initial and final conditions at the Earth and the Moon as defined in the previous section. The initial orbit is a trajectory belonging to the set $\mathcal{E}_{SE}$, whereas the second part is defined using a suitable attainable set. This is made up by tangential low-thrust orbits that are integrated

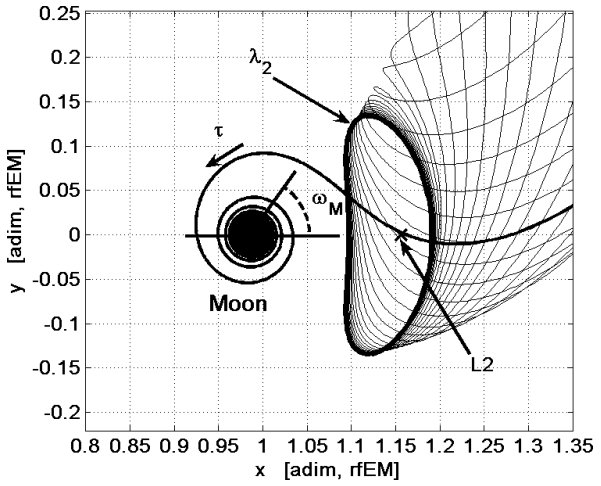

(a) Sample low-thrust capture trajectory.

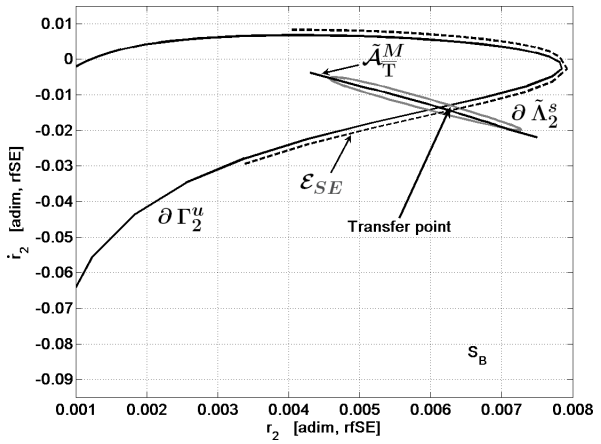

(b) $\mathcal{E}_{SE}$ and $\tilde{\mathcal{A}}^M_{\mathbf{T}}(-t)$ sets.

Fig. 4. The first guess low-thrust capture solution as the transfer point $\mathcal{T}^M_{-t} = \mathcal{E}_{SE} \cap \tilde{\mathcal{A}}^M_{\mathbf{T}}(-t)$, the latter reported on section S_B in Fig. 4(b).

backward. More specifically, as both eccentricity and apsidal altitude are prescribed, the final state of the transfers (i.e. the periapsis point of the orbit about the Moon) is function of the argument of periapsis, i.e. $\mathbf{y}_f = \mathbf{y}_f(\omega_M)$, as shown in Fig. 4(a). The domain of admissible final states therefore is

$$\mathcal{Y}^M = \{\mathbf{y}_f(\omega_M) | \omega_M \in [0, 2\pi]\}, \tag{19}$$

and the attainable set, for some $t \geq 0$ (i.e. $-t$ is a backward integration), containing low-thrust, ballistic capture trajectories is

$$\mathcal{A}^M_{\mathbf{T}}(-t) = \bigcup_{\mathbf{y}_f \in \mathcal{Y}^M} \gamma_{\overline{\mathbf{T}}}(\mathbf{y}_f(\omega_M), -t). \tag{20}$$

Since the first part of the transfer is defined on $\mathcal{E}_{SE}$, the transfer points, if any, that generate low-energy, low-thrust transfers are contained in the set

$$\mathcal{T}^M_{-t} = \mathcal{E}_{SE} \cap \tilde{\mathcal{A}}^M_{\overline{\mathbf{T}}}(-t). \tag{21}$$

The transformation $\mathcal{M}$ is required to map $\mathcal{A}^M_{\mathbf{T}}(-t)$, computed in the EM model, into $\tilde{\mathcal{A}}^M_{\mathbf{T}}(-t)$, defined in the SE model, as shown in Fig. 4(b). It is worth mentioning that first guess solutions are being generated in this step. These preliminary solutions have to be later optimized in a four-body context. Thus, small discontinuities can be tolerated when looking for the transfer point. This means that it is possible to intersect two states such that $\|\mathbf{y}_A - \mathbf{y}_E\| \leq \varepsilon$, where $\mathbf{y}_E \in \mathcal{E}_{SE}$, $\mathbf{y}_A \in \tilde{\mathcal{A}}^M_{\overline{\mathbf{T}}}(-t)$, and ε is a prescribed tolerance. The greater ε is, the higher number of first guess solutions is found; however, ε should be kept sufficiently small to permit the convergence of the subsequent optimization step.

5. TRAJECTORY OPTIMIZATION

Once feasible and efficient first guess solutions are achieved, combining attainable sets with Earth-escape sets, an optimal control problem is stated in the BRFBP framework. The model used to take into account low-thrust propulsion and the gravitational attractions of all the celestial bodies involved in the design process (i.e. the Sun, the Earth, and the Moon) is

$$\begin{aligned} &\ddot{x} - 2\dot{y} = \frac{\partial \Omega_S}{\partial x} + \frac{T_x}{m}, \quad \ddot{y} + 2\dot{x} = \frac{\partial \Omega_S}{\partial y} + \frac{T_y}{m}, \\ &\dot{\theta} = \omega_S, \quad \dot{m} = -\frac{T}{I_{sp}\, g_0}. \end{aligned} \tag{22}$$

This is a modified version of the classic bicircular four-body problem Simó et al. (1995) (see Fig. 2(b)) and, in principle, incorporates the perturbation of the Sun into the Earth–Moon PCRTBP described by (1). The four-body potential Ω_S reads

$$\Omega_S(x, y, \theta) = \Omega(x, y, \mu_{EM}) + \frac{m_S}{r_S} - \frac{m_S}{\rho_S^2}(x \cos\theta + y \sin\theta). \tag{23}$$

The dimensionless physical constants introduced to describe the Sun perturbation are in agreement with those of the EM model. Thus, the distance between the Sun and the Earth–Moon barycenter is $\rho_S = 3.8878 \cdot 10^2$, the mass of the Sun is $m_S = 3.2890 \cdot 10^5$, and its angular velocity with respect to the EM rotating frame is $\omega_S = -9.2518 \cdot 10^{-1}$. The Sun is located at $(\rho_S \cos\theta, \rho_S \sin\theta)$, and therefore the Sun-spacecraft distance is calculated as

$$r_S^2 = (x - \rho_S \cos\theta)^2 + (y - \rho_S \sin\theta)^2. \tag{24}$$

This low-thrust version of the BRFBP is represented by the sixth-order system of differential (22).

The optimal control problem, OCP, is then transcribed into a nonlinear programming, NLP, problem using a direct approach. This method, although suboptimal, generally shows robustness and versatility, and does not require explicit derivation of the necessary conditions of optimality. Moreover, direct approaches offer higher computational efficiency and are less sensitive to variation of the first guess solutions Betts (1998). Furthermore, a multiple shooting scheme is implemented, where the BRFBP dynamics presented by (22) is forward integrated within $N-1$ intervals (in which $[t_i,\, t_f]$ is uniformly split), i.e. the time domain is divided in the form $t_i = t_1 < \cdots < t_N = t_f$, and the solution is discretized over the N grid nodes. The continuity of position, velocity and mass is imposed at their ends Enright and Conway (1992), in the form of defects $\boldsymbol{\eta}_j = \bar{\mathbf{v}}_j - \mathbf{v}_{j+1} = 0$, for $j = 1, \ldots, N-1$. The quantity $\bar{\mathbf{v}}_j$ stands for the result of the integration, i.e. $\bar{\mathbf{v}}_j = \boldsymbol{\phi}(\mathbf{v}_j, \mathbf{p}, t)$, $t_j \leq t_{j+1}$, and is made up of state variables and control variables (i.e. $\mathbf{v}_j = \{\mathbf{y}_j, \mathbf{T}_{j,k}\}^\top$, for $k = 1, \ldots, M-1$). The control law $\mathbf{T}(t)$ is described within each interval by means of cubic spline functions.

Table 1. Two-impulse transfers and low-energy low-thrust transfers to LLOs. A set of impulsive solutions found in literature is reported.

Type	Δv_i [m/s]	Δv_f [m/s]	f_t [adim.]	Δt [days]
sol.1	3169	–	0.675	103
sol.2	3143	650	0.724	88
Yag	3137	718	0.730	44
WSB	3161	677	0.729	90–120
Hoh	3143	848	0.742	5

6. OPTIMIZED TRANSFER SOLUTIONS

In this section the transfer solutions arising from the optimization process are presented. In section 2 two families of trajectories are discussed, according to different types of propulsion system.

6.1 Low Lunar Orbit Trajectories

Optimal two-impulse and low-energy low-thrust solutions are presented. These transfers start from a circular parking orbit at an altitude of $h_E = 167\,\text{km}$ around the Earth, and end at circular orbit around the Moon, at an altitude of $h_M = 100\,\text{km}$. The results are shown in table 1 as follows: the first sol.1 correspond to the low-energy low-thrust transfer, while solution sol.2 represents a two-impulse low-energy transfer. Then, solutions below the horizontal line are some reference impulsive transfers found in literature.

Table 1 is organized as follows: the second column Δv_i stands for the initial impulsive maneuver that inserts the spacecraft onto the translunar trajectory. For the solutions computed in this paper, they are a direct output of the optimization process, described in section 5. The third column Δv_f represents the final impulsive maneuver that permits a stable permanent capture into a circular parking orbit around the Moon. This comes out from the optimization step for sol.2, it is not present for the low-thrust transfers whereas for the reference solutions this term takes into account all the impulsive maneuvers necessary to carry out the transfers except for Δv_i.

The fourth column f_t represents the overall mass fraction necessary to complete the Earth–Moon transfers. Even if for low-energy low-thrust solutions, according to the design of the Earth escape stage described in section 3, the initial Δv_i is given by the launch vehicle, for a sake of a fair comparison, the cost of this maneuver is considered, as written below:

$$f_t = \frac{m_p}{m_i} = \left[1 - \exp\left(-\frac{\Delta v_i}{I_{sp}^{ht}\, g_0}\right)\right] + \frac{1}{m_i}\int_{t_i}^{t_f} \frac{T(t)}{I_{sp}^{lt}\, g_0}\,\mathrm{d}t, \tag{25}$$

where $I_{sp}^{ht} = 300\,\text{s}$ and $I_{sp}^{lt} = 3000\,\text{s}$ are assumed as the specific impulse related to high-thrust chemical engines and low-thrust electrical engines respectively. Finally, the last column on the right stands for the transfer time.

Table 1 shows that sol.1 offers the lowest value of the overall mass consumption (see f_t). This happens for two reasons: first the fact that the low-thrust, I_{sp}^{lt}, is one order of magnitude greater than I_{sp}^{ht}. Second, the first guess solutions exploit deeply the dynamics of the RTBPs where they are designed, and later of the Earth–Moon BRFBP where they are optimized. Moreover, these trajectories take explicitly advantage of the initial lunar flyby. The latter can be seen as a kind of aid in the translunar orbit insertion, as it reduces the Δv_i required for that maneuver. The two-impulse trajectory corresponding to sol.2, shown in Fig. 5, acknowledges these remarks, as it shows the lowest global $\Delta v = 3793\,\text{m/s}$ (with travel time $\Delta t = 88\,\text{days}$).

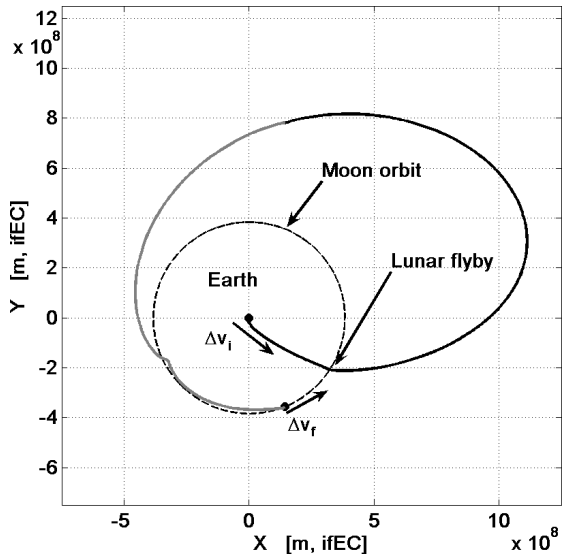

(a) Optimized two-impulse trajectory, inertial geocentric reference frame.

Fig. 5. Optimized two-impulse transfer to a low orbit around the Moon, corresponding to solution 2 in table 1.

7. CONCLUSIONS

In this paper two different technique to design Earth-to-Moon transfers have been investigated. The optimized solutions reveal to be efficient, both in terms of Δv and flight time.

REFERENCES

E.A. Belbruno and J.K. Miller. Sun-Perturbed Earth-to-Moon Transfers with Ballistic Capture. *Journal of Guidance Control and Dynamics*, 16:770–775, 1993.

J.T. Betts. Survey of Numerical Methods for Trajectory Optimization. *Journal of Guidance control and dynamics*, 21(2):193–207, 1998.

P.J. Enright and B.A. Conway. Discrete Approximations to Optimal Trajectories Using Direct Transcription and Nonlinear Programming. *Journal of Guidance Control and Dynamics*, 15:994–1002, 1992.

W. Koon, M. Lo, J. Marsden, and S. Ross. Low Energy Transfer to the Moon. *Celestial Mechanics and Dynamical Astronomy*, 81:63–73, 2001.

C. Simó, G. Gómez, A. Jorba, and J. Masdemont. The Bicircular Model near the Triangular Libration Points of the RTBP. In *From Newton to Chaos*, pages 343–370, 1995.

V. Szebehely. *Theory of Orbits: the Restricted Problem of Three Bodies*. Academic Press New York, 1967.